Experimental Assessment of Generalised Super-Twisting Control for Optimal Reference Tracking in Wave Energy Systems

Experimental Assessment of Generalised Super-Twisting Control for Optimal Reference Tracking in Wave Energy Systems

F.D. Mosquera [*,**] **N. Faedo** [**] **P.F. Puleston** [*]
C.A. Evangelista [*]

[*] *Instituto de Investigaciones en Electrónica, Control y Procesamiento de Señales (LEICI) - Universidad Nacional de La Plata & CONICET, Argentina.*
[**] *Marine Offshore Renewable Energy Lab., Dept. of Mechanical and Aerospace Engineering - Politecnico di Torino, Italy*

Abstract: Maximising wave energy extraction is essential for the successful operation of wave energy converters, and appropriate control strategies play a vital role in achieving this objective. This paper presents a control scheme for an experimental wave energy converter setup. The strategy combines an optimal moment-based reference generation technique with a higher-order sliding mode tracking controller, which provides robust tracking of the associated reference, regardless of the uncertainty present in the experimental operation. The device is tested with two different irregular sea states, and results show that the control structure effectively deals with the system's underlying uncertainty, achieving excellent tracking performance while guiding the system to the corresponding surface following the theoretical phase plot convergence. Furthermore, the comparison with a PID tracking control structure indicates that a proper modification of the tracking element of the loop can improve energy extraction. Finally, consistent tracking error and phase plot evolution behaviour are observed for both sea states.

Keywords: Wave Tank Experiments, Wave Energy Maximisation, Robust Tracking Control, Moment-Based Optimal Control, Higher Order Sliding Modes.

1. INTRODUCTION

Wave energy extraction has a huge potential to help in diversifying renewable energy sources, since it can be combined with solar and wind given the relatively constant availability of wave energy when no sun or wind are present. Nevertheless, the path towards commercialisation of wave energy technology faces a number of unsolved issues (Ringwood, 2020). One topic which requires further development is the control problem for wave energy converters (WECs), which consists in manipulating the load force or torque on the power take-off (PTO) to maximise the captured power, while ensuring that the physical device constraints are not violated (Korde and Ringwood, 2016). In the field of hydrodynamic control techniques for wave energy converters (WECs), Faedo (2020) has developed an optimal control strategy based on moments. This strategy maximizes the energy extracted by the WEC while respecting physical limitations of the system. Here, this control design technique is applied to an experimental WEC by using the optimal reference generated by moment-based control in a feedback control structure. This configuration has previously demonstrated positive results in simulations (Mosquera et al., 2022) and hardware-in-the-loop testing (Faedo et al., 2022b) for various WEC systems. The current study evaluates the control technique in a 1:20 scale prototype of the Wavestar WEC (Hansen and Kramer, 2011) in the Ocean and Coastal Engineering Laboratory wave tank at Aalborg University.

The feedback configuration chosen for the experimental assessment of the control structure is motivated by the large level of uncertainty present in the system under testing. In particular, to track the moment-based optimal reference, a robust control term is required, able to deal both with model uncertainties and potential perturbations. Among the main robust tracking strategies are the sliding mode controllers (SMC), first reported in English by Utkin (1992). This control technique has theoretically exact compensation (insensitivity) of bounded matched uncertainties, a reduction in the order of the system equations, and a finite-time convergence to the sliding surface.

One of the main disadvantages of SMC are the fast oscillations produced in the output of the system, *i.e.* chattering, due to the unmodelled dynamics in the actuator, combined with the discontinuous control action applied directly to the system. Chattering can severely harm mechanical devices so, to attenuate such effect, high-order sliding

[⋆] This project has received funding from the European Union's Horizon 2020 research and innovation programme under the Marie Sklodowska-Curie grant agreement No. 101024372. This research was also supported by the Facultad de Ingeniería, Universidad Nacional de La Plata (UNLP), CONICET and Agencia I+D+i, from Argentina.

modes control (HOSM) techniques have been proposed as a possible solution, where the second order sliding mode (SOSM) has been the most developed. The idea behind these techniques is that the chattering can be reduced if not only the sliding variable goes to zero, but also its derivative. The first algorithm of this family, is the so-called Twisting, proposed by Levant (1987), which applies a discontinuous control action to the second derivative of the sliding variable. The vast majority of the algorithms proposed within this family reduce the chattering in the output substantially (Bartolini et al., 1999), but only can be applied to sliding variables of relative degree 2 with respect to (w.r.t) the control input. Then, a solution to the discontinuous control action has been made available within the family of SOSM for sliding variables of relative degree 1 w.r.t. the control input, with the development of super-twisting algorithm (STA) (Levant, 1993), which employs a continuous control action while retaining the robust characteristics of the SMC. Finally, with the theory of the continuous nested sliding mode algorithms in HOSM, a generalised super-twisting algorithm (GSTA) version has been presented, which can be applied to systems of relative degree r with finite time convergence to the $(r+1)$ order sliding-mode set (Fridman et al., 2015).

Exploiting the improvements developed by the SMC community, and echoing the positive results of GSTA applied to mechanical systems (Borlaug et al., 2021), within this paper, the tracking control term is design and applied in terms of a $3rd$ order GSTA. This term is continuous and guarantees the robust accomplishment of the moment-based reference tracking, reducing any potential mechanical oscillations that could reduce the lifetime of WEC components.

The reminder of the paper is organised as follows. In Sec. 2 the experimental set up, device dimensions, and hydrodynamic model, are presented. Sec. 3 discusses the optimal reference generation, and the tracking control structure utilised. Finally, experimental results and conclusions are depicted in Sec. 4 and 5, respectively.

2. EXPERIMENTAL SETUP - SYSTEM MODEL

In this section, the WEC system utilised for the experimental tests is described. The device is a single degree of freedom (DOF) wave-activated body WEC (Fig. 1). The floater is connected to the fixed reference frame through a hinge (point A). At equilibrium, the floater arm stands at approx. 30° w.r.t the still water line (SWL), see Fig. 1. The submerged volume of the floater resembles a hemisphere in the static position. The system is equipped with the following hardware:

- *Linear Motor and Controller:* LinMot Series P01-37x240F and LinMot E1200.
- *Force Sensor:* s-beam load cell, Futek LSB302 300lb, with SGA Analogue Strain Gauge Amplifier.
- *Position Sensor:* MicroEpsilon ILD-1402-600.
- *Accelerometer:* Dual-axis accelerometer, Analog Devices ADXL203EB.
- *I/O Board:* Speedgoat Performance real time target machine.

Additionally, resistive wave gauges are placed within the tank, to provide real-time information on the free-surface elevation with respect to the still water level (SWL).

The linear motor, which acts as a PTO, provides the system with an effective force, with a constraint in the range of ± 60 [N]. Some relevant dimensions are listed in Table 1, referenced to the $x-z$ axis in Fig. 1. It is important to clarify that linearly measured position and force will be converted to control torque and angular motion in order to design and apply the controller. This frame conversion is made by a trigonometric calculation (Ringwood et al., 2019).

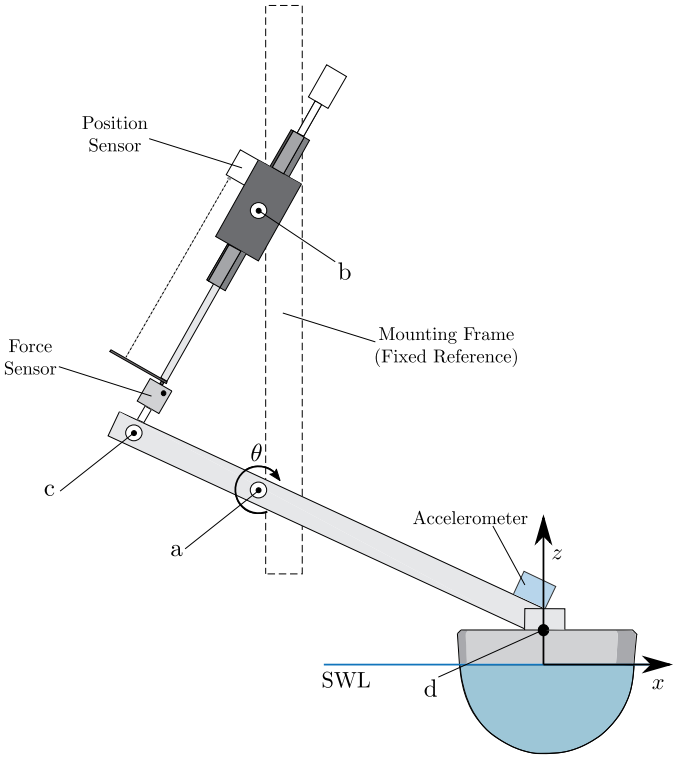

Fig. 1. Schematic of experimental WEC system. Dimensions are in Table 1.

Table 1. Device dimensions and mass properties relative to the SWL.

Parameter	*Value*	*[Unit]*
Float Mass	3.075	[kg]
Float Draft	0.11	[m]
Float Diameter (at SWL)	0.256	[m]
Arm mass	1.157	[kg]
Hinge a (x,z)	(-0.438,0.302)	[m]
Hinge b (x,z)	(-0.438,0.714)	[m]
Hinge c (x,z)	(-0.621,0.382)	[m]

2.1 Control-oriented WEC Hydrodynamic Model

The model for the system is calculated via standard system identification, as in *e.g.* (García-Violini et al., 2021). In particular, a strictly proper, minimal, state-space system is obtained, which can be written as

$$\begin{cases} \dot{x} = Ax + B\left(T_{\mathrm{e}} - u\right), \\ \theta = Cx, \end{cases} \tag{1}$$

here, $x(t) \in \mathbb{R}^n$ is the state vector of a black-box representation, θ the angular position, output of the identified model, and the triplet $(A, B, C^T) \in \mathbb{R}^{n\times n}\times\mathbb{R}^n\times\mathbb{R}^n$ are the dynamic, input, and output matrices, respectively. Finally, T_e is the excitation torque and u is the torque control action.

3. CONTROL STRUCTURE DESIGN

This section presents the design of the control structure and associated controller, see Fig. 2. The latter is comprised by two terms:

$$u = u_{opt} + u_{GSTA}, \tag{2}$$

u_{opt} is the moment-based optimal control action, which is briefly described in Sec. 3.1. This term provides the bulk of the control action, and would make the system work at the optimal operation point in ideal operating conditions (neither uncertainties nor perturbations present). While, in real application conditions, the u_{opt} is capable of leading and maintaining the system in the neighbourhood of the optimal operating region. Additionally, its computational method provides an optimal position reference for the second control term u_{GSTA}.

The GSTA term, designed in Sec. 3.2, deals with uncertainty and any potential perturbation affecting the system, to finally reach and maintain the WEC in maximal energy extraction operation.

3.1 Moment-Based Optimal Controller

As mentioned in Sec. 1, a critical objective for WEC systems is that of maximising the energy extracted. In this subsection, the optimal control action and the associated reference are generated considering the following energy map (Faedo et al., 2021)

$$\mathscr{E} : \dot{\theta}u_{opt} \mapsto \int_{\mathcal{T}} \dot{\theta}u_{opt}\mathrm{d}t, \tag{3}$$

which is maximised for a given time period $\mathcal{T} \subset \mathbb{R}^+$, *i.e.* for which energy absorption of the wave resource is optimal.

The control loop designed in this subsection (see Fig. 2) uses information of the sea-state (*i.e.* wave excitation) affecting the WEC system. In particular, such a controller is designed adopting a moment-based direct optimal control approach (see *e.g.* Faedo et al. (2021, 2022a)): Using the system-theoretic notion of a moment, and its connection to the steady-state output response map in (1), the infinite-dimensional optimal control problem

$$\begin{aligned}(P) : &\max_{(\dot{\theta},u_{opt})} \ \mathscr{E},\\ &\text{subject to:}\\ &\text{WEC dynamics}, x \in \mathcal{X}, u_{opt} \in \mathcal{U}, \forall t \in \mathcal{T},\end{aligned} \tag{4}$$

where the sets $\mathcal{X} \subset \mathbb{R}^n$ (closed) and $\mathcal{U} \subset \mathbb{R}$ (compact) represent state and input constraints, respectively, can be discretised (*i.e.* transcribed) into a finite-dimensional Γ-convex non-linear program (see Faedo et al. (2021)).

Additionally, such parametrisation facilitates an efficient numerical computation of an optimal position reference $t \mapsto \theta_{ref}(t) \in \mathbb{R}$, (approximate) solution of (P), which is fed directly to the inner tracking loop (see Fig. 2).

3.2 HOSM Tracking Control Action

SMC is based on applying a control action whose primary function is to switch between two distinctively different structures related to some predefined manifold. This action produces a new type of system motion called sliding mode, which exists on the manifold. This characteristic results in a remarkable performance, which includes robustness to parameter variations and complete rejection of a certain class of disturbances. Furthermore, the system acquires new dynamical properties which were not present in the original (Kamal et al., 2014).

The sliding manifold is defined as $\sigma(x) = 0$, where σ, called sliding variable, is a function of the states. Adequately designed, allows for the accomplishment of the control objectives when sliding mode is occurring. SMC guarantees robust operation on the sliding manifold, in spite of uncertainty and perturbations.

In particular, to accomplish maximal energy extraction, the sliding variable is selected as:

$$\sigma = \theta_{ref} - \theta, \tag{5}$$

where θ_{ref} is the moment-based reference computed in Sec. 3.1. This sliding variable is of relative degree 2 w.r.t u. According to (1):

$$\ddot{\sigma} = \ddot{\theta}_{ref} - CA^2x - CAB\,T_\mathrm{e} + CABu, \tag{6}$$

where $\ddot{\theta}_{ref}$, T_e, and x are bounded.

The GSTA term of (2), for sliding variables of relative degree 2, has the form (Fridman et al., 2015):

$$\begin{cases} u_{GSTA} = -k_1|\phi|^{1/2}\mathrm{sign}(\phi) + v,\\ \dot{v} = -k_3\mathrm{sign}(\phi)\end{cases} \tag{7}$$

where $\phi = \dot{\sigma} + k_2\lceil\sigma\rfloor^{2/3}$, and the following notation is used, for a real variable $z \in \mathbb{R}$ to a real power $p \in \mathbb{R}$, $\lceil z\rfloor^p = |z|^p\mathrm{sign}(z)$.

The stability analysis for the system when this control action is applied can be performed with the candidate Lyapunov function (Moreno, 2009):

$$V(x) = \Xi P \Xi^T, \text{ where } P = \begin{bmatrix} p_1 & -\frac{p_{12}}{2} & \frac{p_{13}}{2}\\ -\frac{p_{12}}{2} & p_2 & -\frac{p_{23}}{2}\\ \frac{p_{13}}{2} & -\frac{p_{23}}{2} & p_3\end{bmatrix}, \tag{8}$$

and the vector $\Xi^T = \left[\lceil\sigma\rfloor^{2/3}\ \phi\ \lceil v\rfloor^2\right]$. Finally, fulfilling the conditions of Lemma 1 in (Fridman et al., 2015), $V(x)$ satisfies $\dot{V} \leq -\kappa V^{3/4}$, and the gains obtained guide the trajectories of the system to $\sigma = \dot{\sigma} = \ddot{\sigma} = 0$ in finite time, *i.e.* a 3^{rd} order sliding mode. A typical convergence phase plot for this control algorithm can be observed in Fig.3.

4. EXPERIMENTAL RESULTS

This section presents the results of the experimental behaviour obtained with the proposed control structure. This assessment is performed for two different sea states characterised with JONSWAP spectra, generated by the wave tank available at Aalborg University (Table 2 and Fig. 4).

First, the main characteristics of the proposed control structure are analysed. Then, a comparison with the most ubiquitous controller, a proportional-integral-derivative (PID), is presented. Finally, the performances of the designed controller under both sea states are analysed.

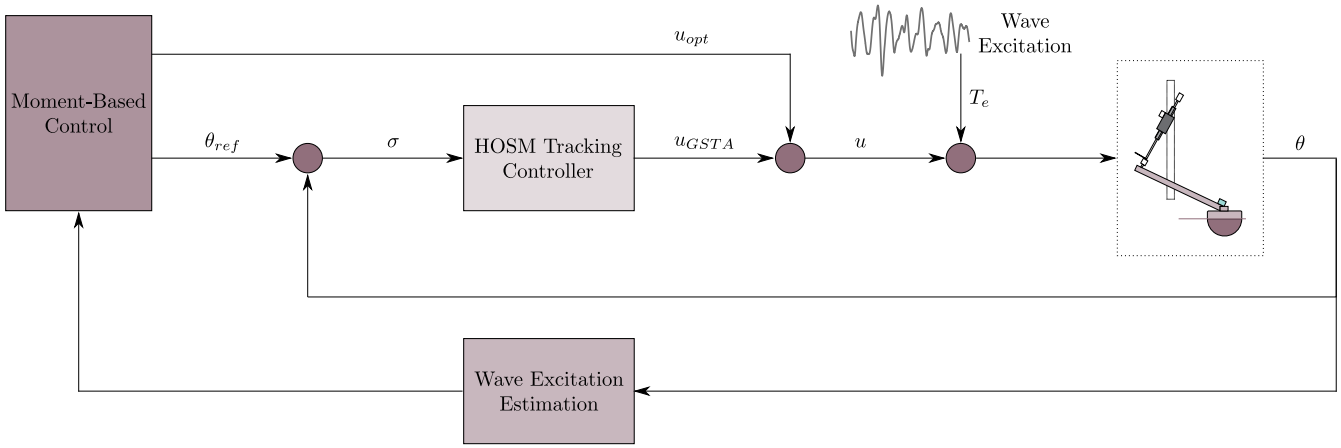

Fig. 2. Control structure schematic.

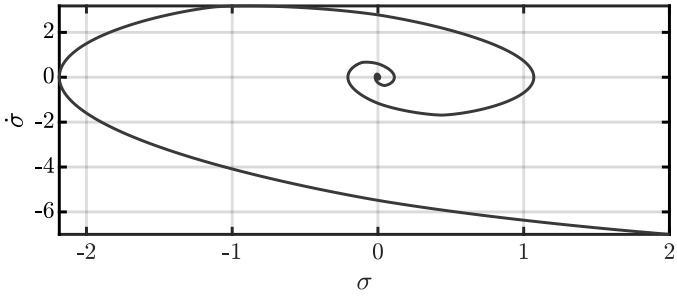

Fig. 3. Example of GSTA convergence to the designed sliding surface for σ of relative degree 2 (Fridman et al., 2015).

Table 2. Sea states considered (Ringwood et al., 2019). H_s, T_p, and γ denote the significant wave height, peak wave period, and peak enhancement factor, respectively.

Sea State	H_s*[m]*	T_p*[s]*	γ
SS1	0.063	1.412	3.3
SS2	0.104	1.836	3.3

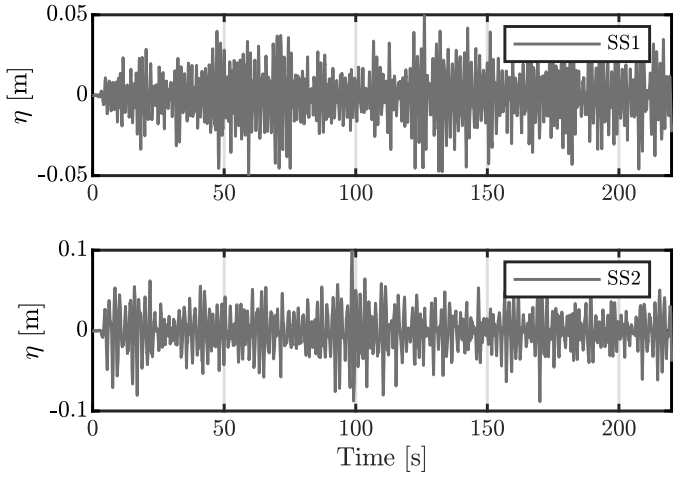

Fig. 4. Wave elevation, η, for the two sea states.

4.1 Analysis of the Control Structure Characteristics

The focus of this subsection is to analyse the behaviour of the control structure in detail. Note that only the results corresponding with SS1 are presented for economy of space, since analogous conclusions stem from SS2. The experimental setup has a control action saturation protection in ±12 [Nm], a sampling frequency of $f_s = 200$ [Hz], and an actuation frequency at $f_a = f_s$.

The optimal control term, u_{opt}, is designed considering the actuator limits within the reference calculation, and, as it can be observed in Fig. 5, the black dashed line, *i.e.* u_{opt}, never exceeds the control limits (dot-dashed line). In additon, the 'complete' control action u, *i.e.* (2), is also indicated in Fig. 5, using a solid line. Note that, within the time intervals in which the optimal control action u_{opt} requires smaller values of torque, a larger control effort of the GSTA term is effectively provided to the system. This can be explained, at least partially, by the correlation between device motion and corresponding control within such intervals: Smaller optimal torque values are correlated with smaller motion requirements, forcing the system to operate in conditions where the (nonlinear) friction associated with the motor becomes relevant, hence departing from the linear representation in (1).

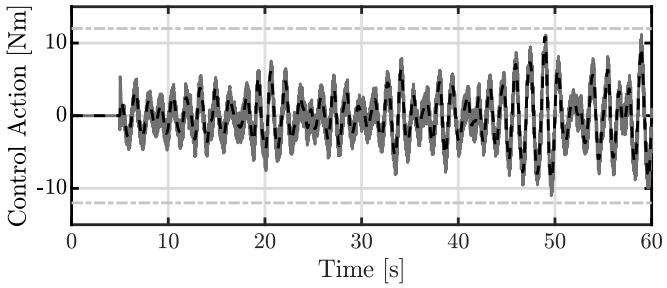

Fig. 5. Total control torque u in solid line, and optimal control torque u_{opt} in dashed line. Saturation level is in dot-dashed line.

Also, in Fig. 5, it can be noticed that the control torque is applied to the system five seconds after the start of the experiment. It is a common practice for allowing system initialisation before application of the control action. As the system is in open loop when the control starts, the working condition differ from the optimal operation point, so u_{GSTA} must guide the trajectories of the system to the designed surface. This behaviour is portrayed in Fig. 6, where the sliding variable and their derivative are guided

to the origin, generating a $3rd$ order sliding mode as discussed in Sec. 3.2. Furthermore, the origin is reached in less than 1 s after the control is activated, while following an analogous phase plot to the theoretical (see Fig. 3).

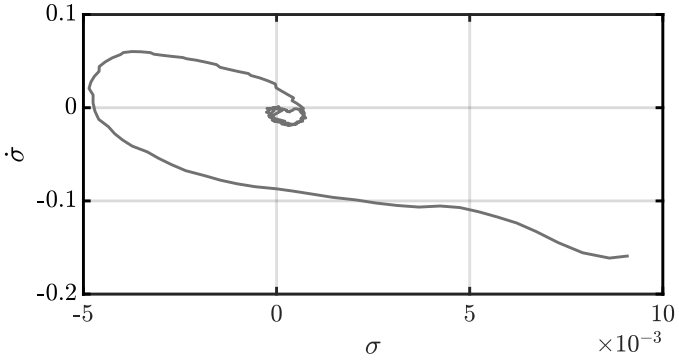

Fig. 6. Experimental convergence to the surface.

On the other hand, the tracking of θ_{ref} for a time window of 60 s is shown in Fig. 7, where a remarkable performance is observed with the tested control structure.

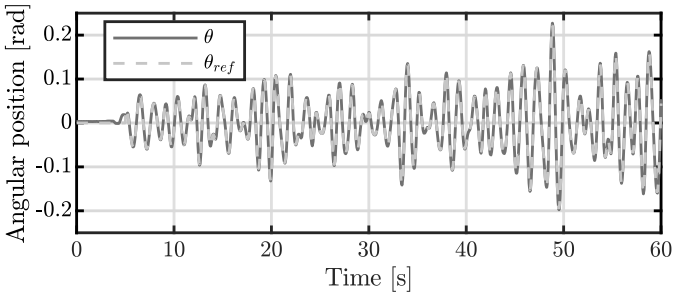

Fig. 7. Reference tracking behaviour for SS1.

4.2 Benchmark Comparison

This subsection provides a comparison with the most well-known controller, *i.e.* the PID, which is selected as a benchmark to contrast with the tracking controller proposed in this paper. The PID is added to the control structure by replacing u_{GSTA} with u_{PID} in (2), *i.e.* $u = u_{opt} + u_{PID}$. As such, the PID is designed as a tracking controller, and its gains are initially adjusted following a Ziegler-Nichols approach, and subsequently tuned heuristically to obtain a fast response with low overshoot.

Fig. 8 compares the absolute error in a logarimic scale for the GSTA and the PID in different gray scales. The absolute error is calculated as $E_i = |\theta_{ref_i} - \theta_i|$. Note that also the mean of these absolute errors are plotted in the figure, as indicated in Fig. 8. It is then straightforward to see that the mean absolute error when the PID controller is used for tracking is 2.5 times larger than the mean absolute error when GSTA is used.

The impact in the tracking performance of this difference can be observed in Fig. 9, which shows the energy extracted by the system when each tracking controller is utilised. Here, around 10% improvement in the extracted energy is obtained for the 4 minutes of experiment duration. This shows the importance of including a robust controller in the tracking loop, which can deal with uncertainty in the system and the tracking requirements.

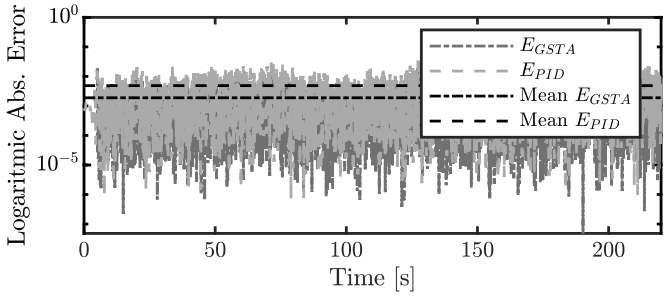

Fig. 8. Logarithmic plot for E_i.

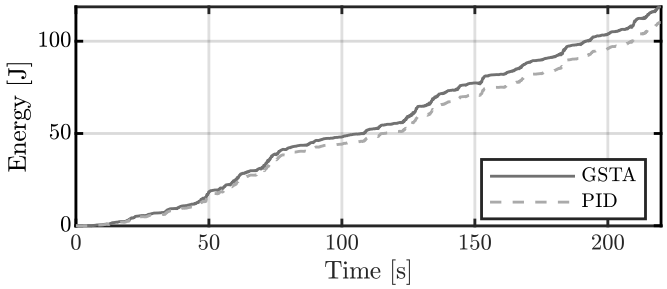

Fig. 9. Energy extraction when applying the GSTA vs. PID.

4.3 Control Structure Evaluated in Other Sea States

The advantages of the GSTA regarding better tracking and robustness are also evaluated in SS2, and the results of both sea states are analysed together.

The tracking performances are compared by computing the relative error $e[\%] = 100\frac{\sum_{i=1}^{n} E_i/n}{\max(\theta_{ref})}$, for each case, in order to fairly contrast the control structure behaviour in sea states which are different in significant height and peak period (see Table 2), the results are in Fig. 10. As expected, the controller performs better with SS1, as the final tuning of the controller is based on this specific sea-state condition. Nevertheless, the difference between relative error in SS1 and SS2 lies around 0.012%, which indicates a high repeatability of the tracking performance for different sea states and associated moment-based optimal references.

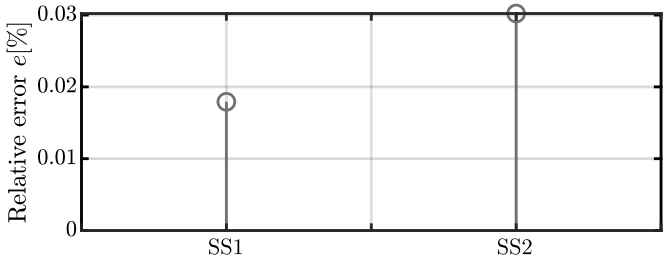

Fig. 10. Relative error of the tracking performance.

Finally, the phase plot convergence to the origin for both sea states is compared in Fig. 11. It is clear that the evolution of the system converges similarly for both sea states. This shows that, even under the different conditions presented in each sea state, the proposed controller moves the system according to similar trajectories, thanks to the inherent robust characteristics of the GSTA term added in the control structure.

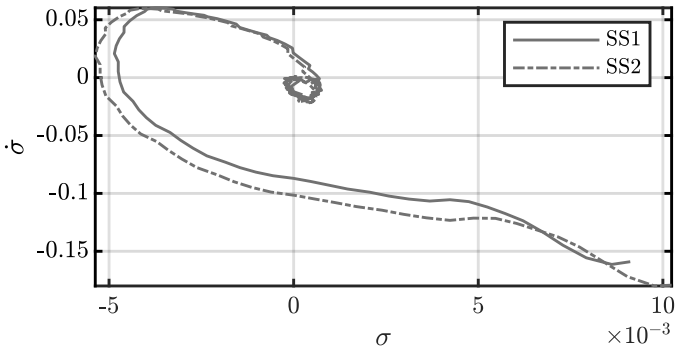

Fig. 11. Phase plot for both sea states.

5. CONCLUSIONS

This paper presents an experimental assessment of a robust optimal position tracking control structure applied to a wave energy converter aiming for energy maximisation. The design combines an optimal moment-based term, with a generalised super-twisting term to deal with uncertainty and perturbations in the system.

Key characteristics are analysed for the proposed control structure with the experimental data obtained. It can be pointed out that the generated computed optimal control effort remains within the protection saturation values of the system, additionally, remarkable tracking of the position reference, and accomplishment of the theoretical predicted trajectory evolution by the experimental system is observed.

Moreover, the generalised super twisting (GSTA) term of the tracking loop is compared against a classical PID. The former showed a better tracking performance and higher energy extraction. Also, the proposed control structure operation is analysed for different sea states and similar behaviour results are obtained.

ACKNOWLEDGEMENTS

Authors would like to thank Prof. Francesco Ferri, PhD. Yerai Peña Sanchez, PhD. students Edoardo Pasta and Guglielmo Papini and all the people involved, for the valuable work made in the experimental campaign in the Aalborg University wave tank.

REFERENCES

Bartolini, G., Ferrara, A., Levant, A., and Usai, E. (1999). On second order sliding mode controllers. In *Var. Struct. Syst. Sliding Mode Nonlinear Control*, 329–350. Springer London, London.

Borlaug, I.L.G., Pettersen, K.Y., and Gravdahl, J.T. (2021). Tracking control of an articulated intervention autonomous underwater vehicle in 6dof using generalized super-twisting: Theory and experiments. *IEEE Transactions on Control Systems Technology*, 29(1), 353–369.

Faedo, N., Giorgi, G., Ringwood, J.V., and Mattiazzo, G. (2022a). Optimal control of wave energy systems considering nonlinear froude–krylov effects: control-oriented modelling and moment-based control. *Nonlinear Dynamics*, 1–28.

Faedo, N., Mosquera, F., Evangelista, C.A., Puleston, P.F., and V., R.J. (2022b). On the preliminary experimental assessment of second-order sliding modes control for wave energy conversion systems. In *Australian and New Zealand Control Conference 2022*.

Faedo, N. (2020). *Optimal control and model reduction for wave energy systems: A moment-based approach*. Ph.D. thesis, Department of Electronic Engineering, Maynooth University.

Faedo, N., Scarciotti, G., Astolfi, A., and Ringwood, J.V. (2021). Nonlinear energy-maximizing optimal control of wave energy systems: A moment-based approach. *IEEE Transactions on Control Systems Technology*, 29(6), 2533–2547.

Fridman, L., Moreno, J.A., Bandyopadhyay, B., Kamal, S., and Chalanga, A. (2015). Continuous nested algorithms: The fifth generation of sliding mode controllers. In *Recent Advances in Sliding Modes: From Control to Intelligent Mechatronics*, 5–35. Springer International Publishing.

García-Violini, D., Peña-Sanchez, Y., Faedo, N., Windt, C., Ferri, F., and Ringwood, J.V. (2021). Experimental implementation and validation of a broadband LTI energy-maximizing control strategy for the wavestar device. *IEEE Transactions on Control Systems Technology*, 29(6), 2609–2621.

Hansen, R.H. and Kramer, M.M. (2011). Modelling and control of the Wavestar prototype. In *Proceedings of the 9th European Wave and Tidal Energy Conference, EWTEC 2011*. University of Southampton.

Kamal, S., Chalanga, A., Moreno, J.A., Fridman, L., and Bandyopadhyay, B. (2014). Higher order super-twisting algorithm. In *2014 13th International Workshop on Variable Structure Systems (VSS)*, 1–5. IEEE.

Korde, U.A. and Ringwood, J.V. (2016). *Hydrodynamic Control of Wave Energy Devices*. Cambridge U. Press.

Levant, A. (1987). *Higher-order sliding modes and their application in control of uncertain processes (in Russian)*. Ph.D. thesis, Institute for System Studies of the USSR Academy of Sciences, Moscow.

Levant, A. (1993). Sliding order and sliding accuracy in sliding mode control. *Int. J. Control*, 58(6), 1247–1263.

Moreno, J.A. (2009). A linear framework for the robust stability analysis of a generalized super-twisting algorithm. In *2009 6th International Conference on Electrical Engineering, Computing Science and Automatic Control (CCE)*, 1–6.

Mosquera, F., Faedo, N., Evangelista, C.A., Puleston, P.F., and Ringwood, J.V. (2022). Energy-maximising tracking control for a nonlinear heaving point absorber system commanded by second order sliding modes. In *14th IFAC Conference on Control Applications in Marine Systems, Robotics and Vehicles, Lyngby, Denmark*.

Ringwood, J., Ferri, F., Tom, N., Ruehl, K., Faedo, N., Bacelli, G., Yu, Y.H., and Coe, R.G. (2019). The wave energy converter control competition: Overview. In *Int. Conf. on Offshore Mechanics and Arctic Engineering*. American Society of Mechanical Engineers.

Ringwood, J.V. (2020). Wave energy control: status and perspectives 2020. *IFAC-PapersOnLine*, 53(2), 12271–12282.

Utkin, V.I. (1992). *Sliding Modes in Control and Optimization*. Springer-Verlag, Berlin, Germany.